Nanoscale Advances

ROYAL SOCIETY OF CHEMISTRY

PAPER

View Article Online
View Journal | View Issue

Cite this: *Nanoscale Adv.*, 2024, **6**, 4877

Scalable and adaptable two-ligand co-solvent transfer methodology for gold bipyramids to organic solvents†

Caitlin D. Coplan, [a] Nicolas E. Watkins, [a] Xiao-Min Lin [b] and Richard D. Schaller *[ab]

Large and faceted nanoparticles, such as gold bipyramids, presently require synthesis using alkyl ammonium halide ligands in aqueous conditions to stabilize the structure, which impedes subsequent transfer and suspension of such nanoparticles in low polarity solvents despite success with few nanometer gold nanoparticles of shapes such as spheres. Phase transfer methodologies present a feasible avenue to maintain colloidal stability of suspensions and move high surface energy particles into organic solvent environments. Here, we present a method to yield stable suspensions of gold bipyramids in low-polarity solvents, including methanol, dimethylformamide, chloroform, and toluene, through the requisite combination of two capping agents and the presence of a co-solvent. By utilizing PEG-SH functionalization for stability, dodecanethiol (DDT) as the organic-soluble capping agent, and methanol to aid in the phase transfer, gold bipyramids with a wide-range of aspect ratios and sizes can be transferred between water and chloroform readily and maintain colloidal stability. Subsequent transfer to various organic and low-polarity solvents is then demonstrated for the first time.

Received 26th June 2024
Accepted 19th July 2024

DOI: 10.1039/d4na00527a

rsc.li/nanoscale-advances

Introduction

Significant attention has focused on the synthesis, processing, and application of metal nanoparticles due to the emergent physical properties they exhibit compared to the bulk. In particular, noble metal nanoparticles can support localized surface plasmon resonances (LSPRs) across a wide range of wavelengths.[1] These LSPRs exhibit strong coupling to light and can be tailored based on the choice of material, size, shape, and dielectric environment, allowing for broad tunability. This control facilitates prospective implementation in wide-ranging applications that span absorption cross-section enhancements in solar energy conversion devices[2–5] and novel optical chromophores through hybridization of plasmons with excitons[6–8] to bio- and chemical sensing.[9–15] However, each of these approaches requires proximity of the plasmonic particles to other chemical species, and the development of such interactions often requires co-miscibility of constituent species. There also exists the limitations of biological applications related to the toxicity or interaction of ligands.[16,17]

With commonly used metal precursors, reducing agents, and ligands, typical solvents chosen for metal particle syntheses must be polar and, most often, aqueous. While studies have probed the ability to synthesize various noble metal nanoparticles in non-polar environments,[18] phase transfer of nanoparticles after synthesis has remained an effective method of creating stable colloidal suspensions of noble metal nanoparticles in low-polarity liquids.

While many of the initial phase transfer methods were demonstrated for small (typically less than 5 nm), spherical nanoparticles, these approaches often failed when applied to larger particle sizes and non-spherical or faceted shapes. This was partly due to the increased total surface energy of the particles and decreased stability in solution.[19–21] Strongly bound ligands such as cetyltrimethylammonium bromide (CTAB) or chloride (CTAC), which facilitate synthesis of gold nanoparticles such as nanorods (NRs) and bipyramids (BPs), present additional challenges, chiefly that these ligands are challenging to displace entirely while maintaining colloidal stability during the ligand displacement process.[19,20,22–27] AuNRs and AuBPs represent key targets of surface exchange owing to aspect ratio shape-tuning, large extinction cross-section plasmonic properties, and demonstrated utility for applications.[23,28,29]

While AuNRs were synthesized successfully without using CTAB as the ligand, the uniformity of the sample suffered due to the shape-directing contribution from the CTA+ counter ion during synthesis.[30] Syntheses of AuBPs available to date have necessitated the presence of CTAB, complicating phase transfer

[a]*Department of Chemistry, Northwestern University, Evanston, IL 60208, USA. E-mail: schaller@northwestern.edu*

[b]*Center for Nanoscale Materials, Argonne National Laboratory, Lemont, IL 60439, USA. E-mail: schaller@anl.gov*

† Electronic supplementary information (ESI) available: Additional experimental details, materials, and methods, including photographs of experimental setup. See DOI: https://doi.org/10.1039/d4na00527a

of this class of nanoparticles.[31–33] As such, AuBPs present a uniquely arduous challenge to successfully transfer from the aqueous into organic phase due to size, shape, and as-synthesized ligand.

To overcome these described issues, ligand-exchange methods utilizing liquid–liquid interface phase transfer have proven useful in various approaches, including introducing co-solvents and exposing particles to two exchange-mediating ligands simultaneously or in succession.[22,34,35] A method commonly used in facilitating nanoparticle phase transfer is co-solvent phase transfer, which utilizes a third solvent that is both miscible with water and the desired organic solvent to increase nanoparticle dispersibility.[19,36,37] Methods using two ligand exchange steps allow for the displacement and stabilization of the nanoparticles in the aqueous phase with a weaker binding affinity than the CTAB ligand, which allows for more facile phase transfer, such as using organic, hydrophobic alkylthiol ligands in a second ligand exchange step.[20,38] For the case of CTAB and other strongly bound ligands, the presence of a co-solvent increases the critical micelle concentration, thus destabilizing the CTAB ligand layer around the nanoparticle and supporting CTAB displacement.[37,39]

Here, we report the development and adaptation of phase transfer techniques to successfully transfer AuBPs in organic suspension with high stability and throughput, which, to our knowledge, has yet to be reported for this particle shape for such a wide range of solvents. Having failed to apply published strategies that are successful for other gold nanostructures such as spheres and nanorods, we develop a combined two-ligand, co-solvent transfer methodology, resulting in rapid and robust phase transfer of AuBPs. We also report on the subsequent processing through centrifugation and re-suspension into a wide range of organic solvents. This approach provides a robust means to phase transfer to various solvents ranging in polarity, thus expanding the potential applications of AuBPs for interactions with other materials and systems that were not previously accessible in the aqueous phase. Transfer of AuBPs into organic solvents will also prove beneficial for creating dispersed monolayers of nanoparticles for further wide-ranging applications within catalysis, sensing, and photovoltaics. Further manipulation after transfer to organics for biologically relevant applications could also be interrogated,[40] due to the high throughput of this phase transfer methodology.

Results and discussion

Initial experiments we performed targeted phase transfer using only a co-solvent with methanol and using a thiolated PEG for stabilization, which can be seen in Fig. S1.† While there was successful transfer of AuBPs into the organic phase through following the reported procedure,[19] aggregation was discernible by eye and was spectroscopically detectable. Also of note were the relatively short shelf-life of the samples, on the order of hours, before loss of colloidal stability.

Subsequent exchange attempts focused on other routes of phase transfer. We pursued a two transfer ligand system of PEG-SH in the aqueous phase and DDT in the organic phase.[20] Many attempts of this approach were carried out, all leading to severe aggregation of the AuBPs at the interface of the two solvents. Extended agitation also did not improve results. Notably, use of just one of the ligands (PEG-SH or DDT), or the mixing of the AuBPs in the aqueous PEG-SH solution and organic DDT solution, even with vigorous mixing, did not result in successful phase transfer. This may suggest the high surface energy of the AuBPs, due to large size and sharp tips, require more facilitation to transfer and maintain stability in the organic phase than even similarly sized AuNRs require.[19,20]

A combination of the above two methods, use of two transfer ligands and a co-solvent, was carried out and resulted in complete phase transfer with the highest yield possible *via* a simple and efficient methodology. This transfer method yielded both visually (through visible color change), and spectroscopically (using UV-Vis) discernible transfer. In particular, the following successful phase transfer method used both PEG-SH and DDT as phase-transfer ligands together with the aid of a co-solvent, methanol.

Typically, 1 mL of the as-synthesized AuBP samples in water were centrifuged at 8000 rpm for at least 15 minutes and then re-suspended using 1 mL of 0.5 mg mL^{-1} (0.1 mM) solution of a 6000 M.W. PEG-SH in MilliQ water. This was then left to sit for one hour to allow for ligand exchange and improved phase transfer. The aqueous AuBP solution was then combined with an equal volume of a 10 mM DDT solution in chloroform in a capped centrifuge tube, inverted a few times, and left to sit for another 20 minutes, which improved overall phase transfer. A co-solvent was then added in equivalent volumes, mixed piecewise until only one homogeneous liquid phase was observed, often after the addition of five equivalent volumes total. MilliQ water was then added until all color appeared in the bottom phase (organic) and the liquids were left to settle (indicated by the opacity of the top aqueous layer). The aqueous layer was then separated from the organic layer using Pasteur pipetting or decanting. A schematic outlining this procedure is shown in Fig. 1 in steps 1–4.

Using this general methodology, a range of DDT concentrations for a constant concentration of PEG-SH (0.1 mM) was investigated probing successful transfer of AuBPs into the organic phase from 10 mM to 100 mM DDT. Within this range, there were only slight variations in transfer efficiency, with 10 mM DDT solutions being chosen for this report.

Care was taken to examine the possibility of phase transfer with PEG molecules of a similar molecular weight but lacking the single thiol moiety. We wished to determine whether the PEG-SH anchors to the surface of the AuBPs, and thus aids in ligand binding during transfer, or determine if micelles of AuBPs still retaining synthetic ligands remained. We examined two non-thiolated PEG molecules and multiple trials were carried out for both lower (4000) and higher (8000) molecular weight PEG, which all led to severe AuBP aggregation and loss of colloidally stable solution (Fig. S2†). These observations agree with the results shown for AuNRs by Alkilany *et al.*[19] and strongly suggests that the thiol group is necessary and does attach to the gold surface, and is inconsistent with reverse micelle encapsulation.

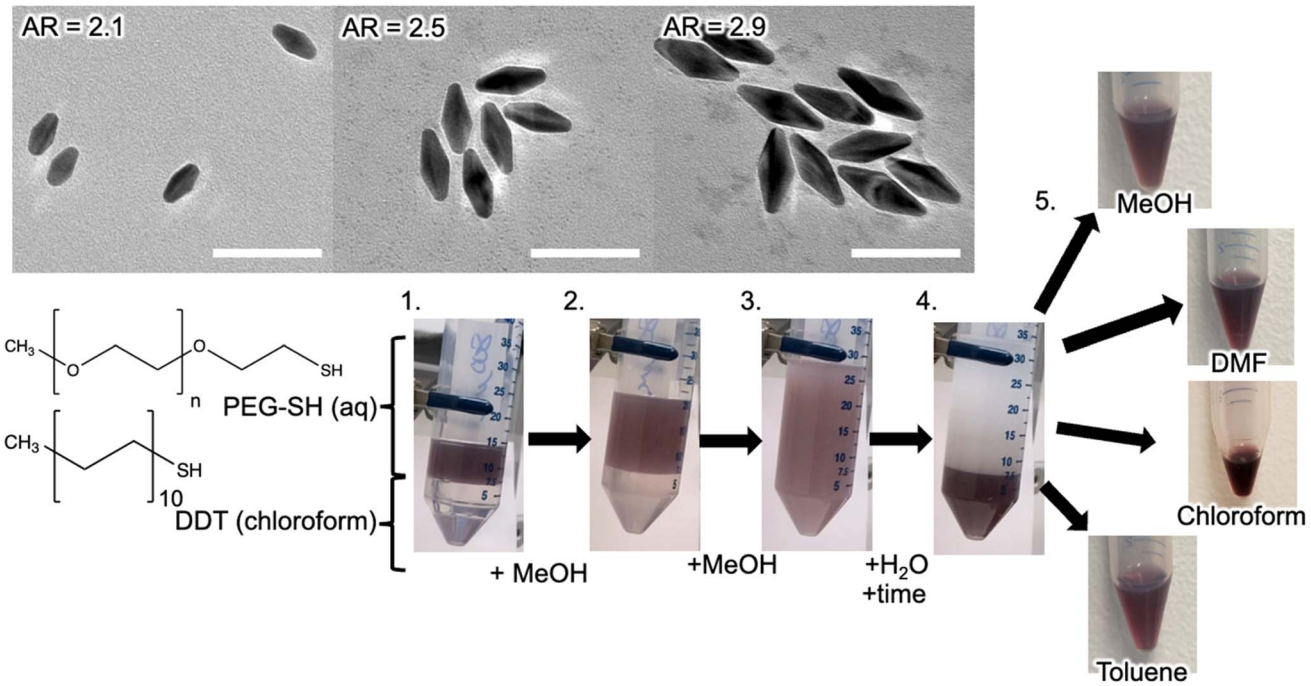

Fig. 1 Schematic of the combined co-solvent and two-ligand system, utilizing PEG-SH in the aqueous phase and DDT in the organic phase with MeOH as the co-solvent of choice. A range of AuBP aspect ratios were examined, ranging from 2.1 (left), 2.5 (middle), and 2.9 (right). All scale bars for TEM images are 100 nm. (1) The solutions of AuBPs and PEG-SH are added to a DDT in chloroform solution. (2) Co-solvent methanol is added in volume equivalents to the starting volume of aqueous and chloroform solutions piecewise, inverted, and degassed. (3) A total of 5 equivalents of methanol is added until solutions are homogenized. (4) Water is added to aid in separation of aqueous and organic phases again, with the AuBPs subsequently in the organic phase. Over time, the organic AuBP solution settles. (5) The remaining aqueous phase is removed and (if desired), samples can be centrifuged and re-diluted in a variety of end solvents.

Choice of co-solvent was found to be another key component to a successful and stable AuBP phase transfer. As pointed-out in previous works, the co-solvent, which is highly miscible in both liquid phases (here water and chloroform), is necessary for facilitating a spontaneous transfer.[19,36,37] Methanol, ethanol, DMF, DMSO, and IPA served successfully as co-solvents, while acetone and acetonitrile were unsuccessful (Fig. S3†). For the successful co-solvents listed, methanol exhibited the best transfer efficiency, demonstrating an increase in concentration of AuBPs in the organic phase while IPA was the least effective. This can be seen through visual inspection (Fig. 2a) and UV-Vis analysis of each resultant AuBP solution (Fig. 2b and c). The stability of each chloroform AuBP solution was examined for each of the successful co-solvents over the span of 5 days. Each solution demonstrated nearly identical spectra over the first two days, but further sample degradation was evident in following days, due to aggregation of the higher surface energy AuBPs evident in the broadening and shifts of the LSPR peaks (Fig. S4–S6†). These samples moved into organic phase using different co-solvents were found to exhibit peak broadening and peak shifts over time (Fig. S7–S11†). Methanol, shown in Fig. 2c, exhibited the best sample longevity and extinction lineshape retention, followed closely by DMSO (Table S1†). Together, these results suggest that the highly polar protic solvents (MeOH) and polar aprotic solvents (DMSO) are ideal co-solvents. Methanol was chosen as the co-solvent in subsequent experiments.

Following these phase transfer conditions from water to chloroform, successive transfers to other organic solvents were carried out to expand the scope and utility of this methodology. After the transfer procedure outlined above, the dispersion of AuBPs in chloroform was centrifuged at 8000 rpm for 15 minutes and redispersed in a range of organic solvents that were then monitored over the course of a few days (Fig. 1). Immediately following transfer, organic solvents ranging in polarity demonstrated successful suspension of AuBPs, with minimal lineshape changes and spectral shifts that were consistent with refractive indices changes of the effective medium[15] (Fig. 3). Solutions that supported the AuBP suspension included a variety of alcohols (methanol, ethanol, and isopropanol), acetonitrile, acetone, dimethylformamide, dimethyl sulfoxide, and toluene. Hexanes were also examined but resulted in rapid aggregation of the AuBPs (Fig. 4).

These same AuBP samples were tracked over the course of a week both visually (Fig. S12†) and spectroscopically (Fig. S13–S15†). During this time, each sample exhibited absorbance reduction and peak broadening, suggesting aggregation out of solution and possible development of sample inhomogeneities, respectively. A decrease in the ratio of long axis (LA) to short axis (SA) peaks was found for all samples along with the general absorption reduction. Some samples (DMF, DMSO) also

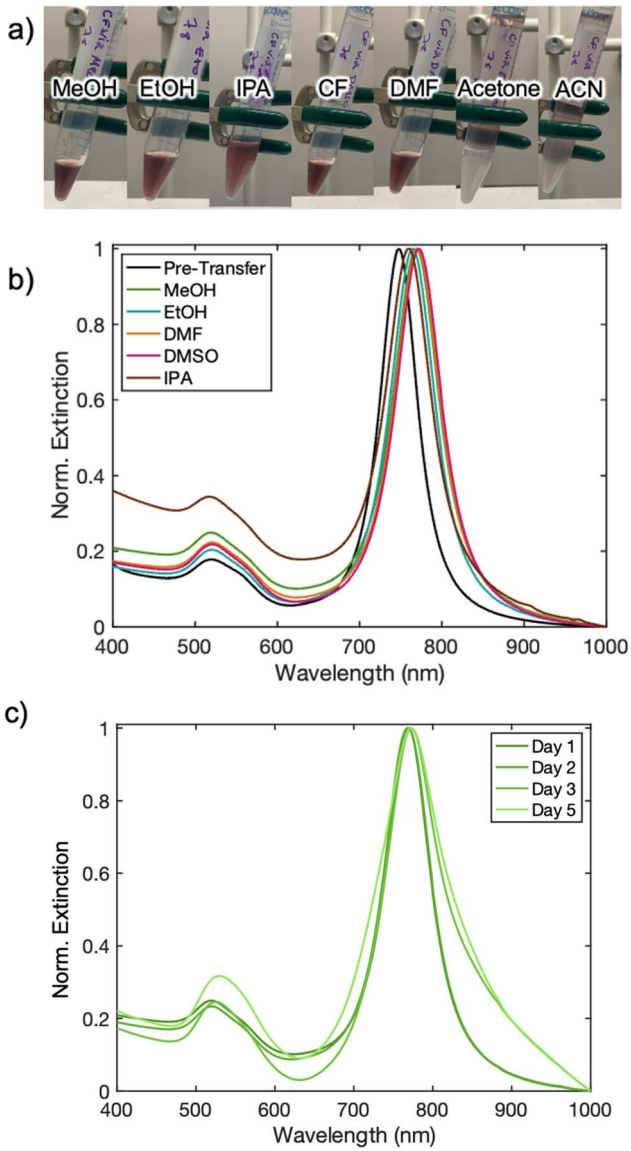

Fig. 2 (a) AuBP phase transfer comparison for different successful co-solvents from left to right include methanol, ethanol, isopropanol, dimethyl sulfoxide, and dimethylformamide. Following these are the attempted solvents that did not work, acetone and acetonitrile. (b) Normalized extinction spectra for each of the successful co-solvent trials. (c) Normalized extinction spectra for methanol as the co-solvent, which exhibited the highest quality AuBP samples over time.

featured significant peak red-shifting, an indicator of agglomeration, by the end of the week trial. All peak changes were tabulated and included in Table S2.†

Four select solvents (chloroform, DMF, MeOH, and toluene) were plotted over time to track peak changes (Fig. S16–S19†). While both chloroform and DMF exhibit excellent initial stability for AuBP solutions, toluene and methanol maintain their good stability over longer periods of time, as exhibited in Table S2.† While it is ideal to use the phase-transferred AuBP samples quickly following redispersion or even after a couple days, samples can be made and used up to a week after redispersion in a wide range of organic solvents.

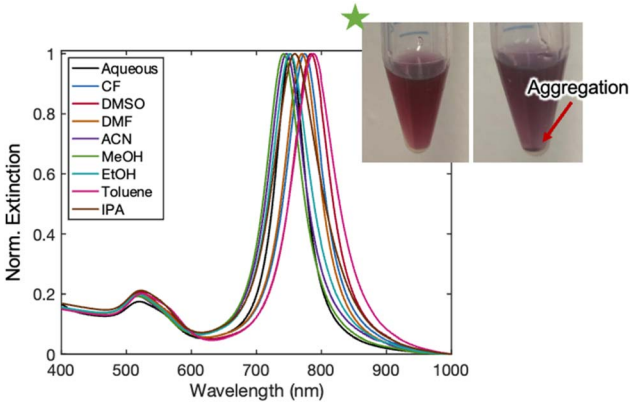

Fig. 3 Normalized extinction spectra for the range of end solvents examined for AuBP samples. All solvents included were successful in creating a stable suspension to varying extents, as demonstrated by the inset photographs of AuBPs in chloroform (left, green star) and in isopropanol (right).

A final set of experiments were completed on the samples using Fourier Transform Infrared (FTIR) spectroscopy to better understand the ligand mixture on the surfaces of the AuBPs. To reduce strong absorbance of solvents within the IR region (as seen in Fig. S20†), sample preparation involved drying of concentrated pellets for low-volatility samples, or using high-volatility solvents. Prior to any functionalization, the AuBPs are clearly functionalized with CTAB alone (Fig. S21a†) and following incubation in the PEG-SH solution, a mixture of CTAB and thiolated-PEG are observed (Fig. S21b†). Determination of exact ligand amount through this technique was not possible, due to many overlapping peaks, however, lineshapes tended toward DDT or PEG-SH depending most likely on ligand solubility in different final solvent selection. This is seen in the comparison of FTIR spectra of AuBP samples evaporated from chloroform (Fig. S22†) and toluene (Fig. S23†).

To further evaluate our methodology, a range of AuBP sizes and aspect ratios (AR) (Fig. S24†) were transferred to a select set of solvents (methanol, DMF, and toluene). AuBPs with AR ranging from 2.1 to 2.9 (Table S3†) were synthesized, transferred to the select set of solvents, and examined using UV-Vis spectroscopy (Fig. 5). Each AuBP AR sample was successfully transferred to each of these solvents with stability in-line with the prior experiments. The highest throughput of AuBP was found with chloroform and DMF as a solvent immediately following AuBP suspension while AuBP samples in methanol and toluene exhibited a consistent suspension of AuBPs over a larger timespan (Fig. S25†) These results confirm applicability of our phase transfer and subsequent suspension of a range of AuBP ARs into many organic solvents.

Conclusions

We have shown the ability to transfer AuBPs into organic solvents using a combination of two exchange ligands combined with a co-solvent method. Through this transfer, we found that AuBPs can be successfully moved from aqueous

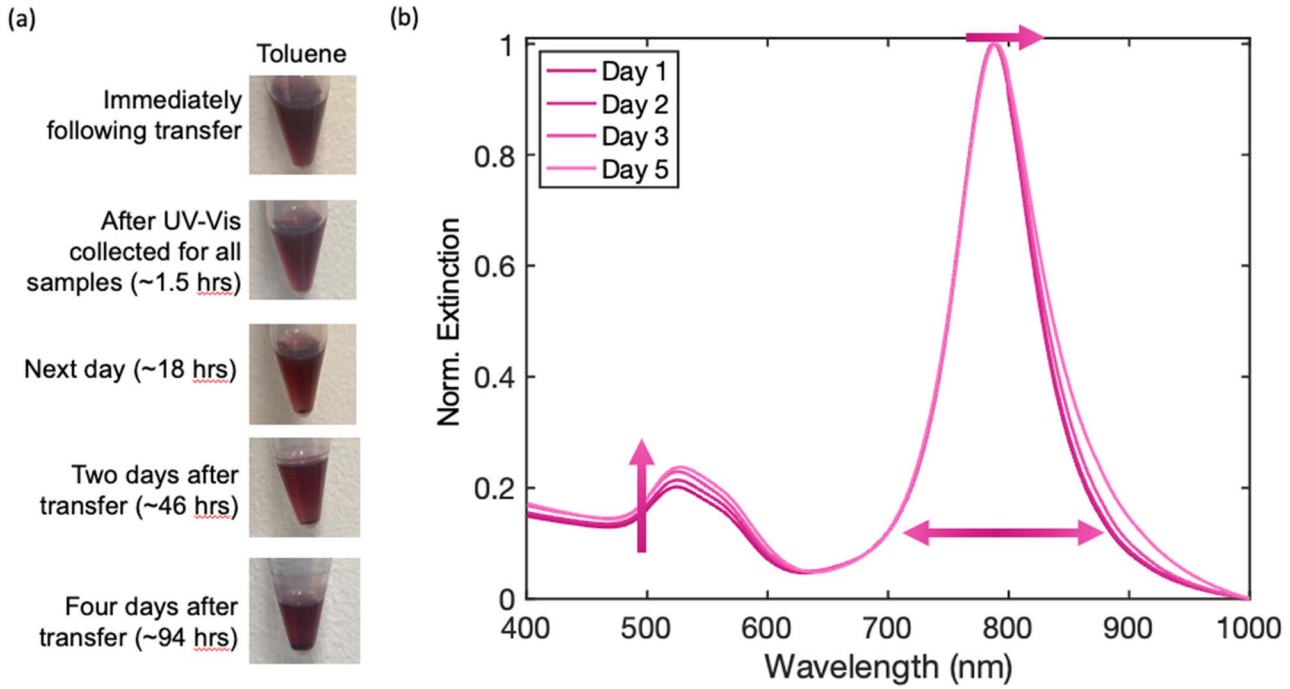

Fig. 4 Visual and spectral data for AuBP sample transferred into toluene as the end solvent. (a) Photographs of AuBP sample in falcon tube. (b) Normalized UV-Vis spectra for corresponding AuBP sample in toluene, exhibiting a relative peak broadening, and red-shift of the long-axis peak, suggesting a slight reduction in stability over time.

suspension to a range of solvents with stabilities ranging from hours to days. We have also shown the impact solvent transfer has on the AuBPs through LSPR peak changes in UV-Vis extinction spectroscopy. First steps of surface characterization could be built upon to identify surface chemistry trends within different end solvents. Future work involving complex solution systems, particularly those that mimic biologically relevant systems, as well as functionalization using bio-molecules offer other interesting pathways to understanding the surface chemistries at play. Transferring these nanoparticles will allow for incorporation into new hybrid material systems, including those requiring non-polar solvents or involving water-sensitive materials. Transfer into these new solvents can also aid in creating a more uniform deposition of the AuBPs on surfaces for surface-enhanced spectroscopic applications in future studies.

Experimental methods

Materials

All aqueous solutions were made using MilliQ (18.2 MΩ cm) water purified using MilliQ IQ 7000 Ultrapure Lab Water System (Millipore Sigma, Merck KGaA, Germany). Gold(III) chloride solution ($HAuCl_4$ 30 wt% in dilute HCl), sodium hydroxide (NaOH, BioXtra, ≥98% pellets, anhydrous), sodium borohydride ($NaBH_4$, Aldrich, powder, ≥98%), citric acid ($HOC(CH_2CO_2H)_2$, ACS Reagent, ≥99.5%), cetyltrimethylammonium chloride (CTAC, 25 wt% in H_2O), cetyltrimethylammonium bromide (CTAB, for molecular biology, ≥99%), silver nitrate ($AgNO_3$, ACS Reagent, ≥99%), 8-hydroxyquinoline (HQL, ACS Reagent, 99%) were purchased from Sigma Aldrich. Nitric acid (HNO_3, 12 M) was purchased from Fischer Scientific. Transfer ligand solutions dodecanethiol (DDT, Aldrich, ≥98%) and poly(ethylene glycol) methyl ether thiol (PEG-SH, Aldrich, average MW 6000) were made as organic or aqueous solutions, respectively. Centrifugation was performed using an Allegra X-30R (Beckman–Coulter, USA). UV-Vis extinction spectra were collected using a Cary 5000 (Agilent, USA). Transmission electron microscopy (TEM) images were collected using a JEOL 2700F operating at 200 kV. TEM grids were prepared by drop casting AuBPs onto 300 mesh grids (Ted Pella) and subsequent rinsing in ethanol for 10 minutes to reduce grid contamination with excess reagents from the solution. AuBP geometries were evaluated using ImageJ. FTIR data were collected at room temperature on a Bruker Tensor 37 FTIR Spectrometer equipped with a Mid IR detector and KBr beam splitter. The spectrum was collected in attenuated total reflectance (ATR) mode in the range of 4000 to 600 cm^{-1}. The data were averaged over 64 scans. The OPUS software was used for the data acquisition, and reference scans were collected between each sample.

Preparation of solutions

$HAuCl_4$, $NaOH{\cdot}NaBH_4$, citric acid, CTAC, CTAB, $AgNO_3$, HNO_3, and PEG-SH solutions were prepared using MilliQ water. HQL solutions were made using 200 proof ethanol. All the above solutions were prepared and stored in plastic centrifuge tubes. DDT solutions were prepared using chloroform and stored in scintillation vials to prevent solvent evaporation.

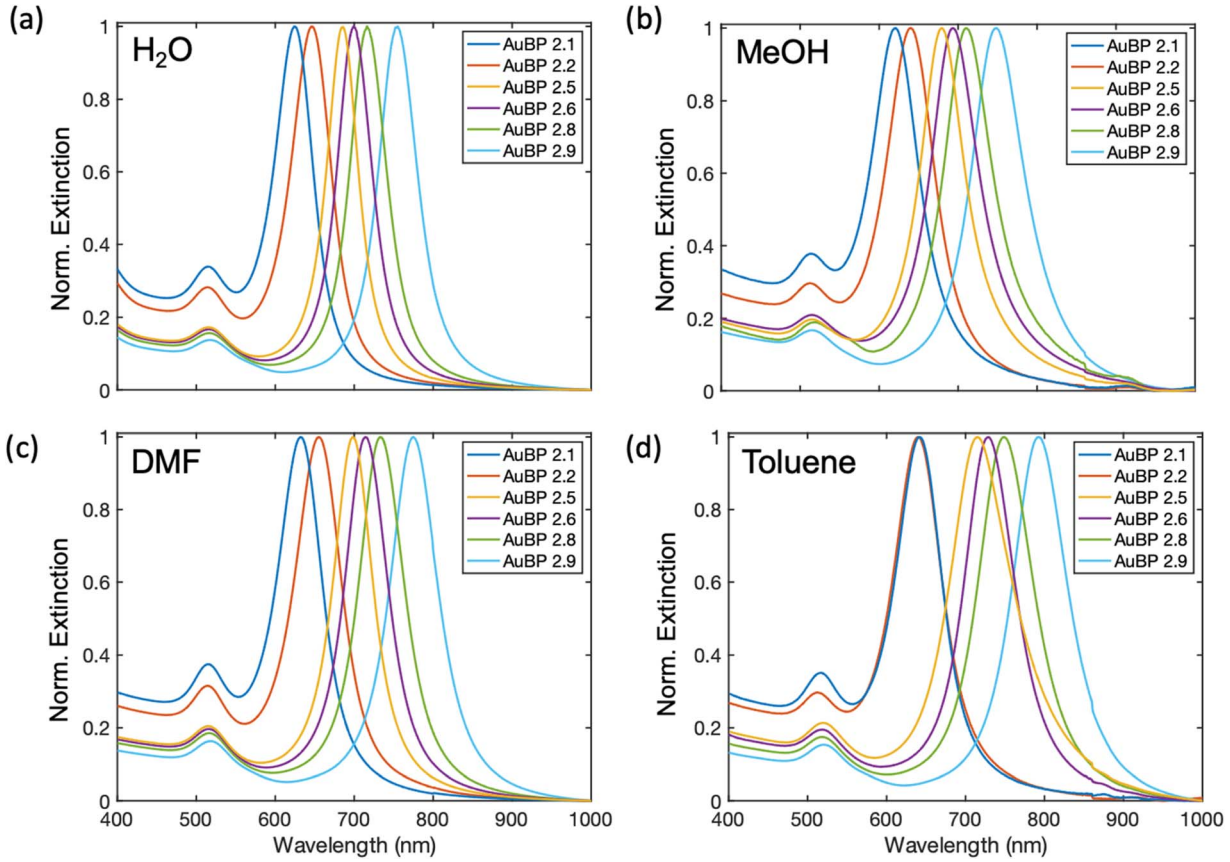

Fig. 5 Normalized extinction spectra for a range of AuBP suspensions in (a) water with CTAB ligand, (b) methanol with DDT and PEGSH ligands, (c) dimethylformamide with DDT and PEGSH ligands, and (d) toluene with DDT and PEGSH ligands immediately following solvent transfer. Legends specify aspect ratio, length to width measurements, of the AuBP suspended in each solvent.

Synthesis of AuBPs

Briefly, AuBPs were synthesized using the seed-mediated method as reported previously by Chateau *et al.*[41] with minor adjustments for increased AuBP-to-biproduct yield as fully detailed in the ESI.† Briefly, gold seed particles are synthesized using a basic solution of sodium borohydride ($NaBH_4$) that reduces $HAuCl_4$ in the presence of citric acid and the capping agent CTAC in an all-aqueous environment. This mixture is heated to 80 °C for two hours with gentle stirring. The seeds are then removed from the bath and stored for use after a 24 hour minimum ageing period (maximum is about 1 month under ambient storage conditions). Following seed synthesis, AuBPs are formed through a growth step where a more concentrated solution of $HAuCl_4$ is reduced by HQL in the presence of $AgNO_3$, CTAB capping agent, and an all-aqueous environment. After rapid stirring for one-minute, various volumes of Au seeds were added, the vial containing the solution was capped, and added to a water bath at 40–50 °C for 15 minutes (CAUTION: Heating of a sealed container can build dangerous pressure in principle). An additional small aliquot of HQL was added after 15 minutes, and the AuBP solution was then added back to the water bath for an additional 30–45 minutes with gentle stirring. AuBP solutions were subsequently allowed to cool to room temperature and then processed by centrifugation at 8000 rpm (approx. 6667 g) for at least 15 minutes to remove excess surfactant and reagent molecules, followed by re-diluted using 18.2 MΩ cm (MilliQ) water to produce deep maroon suspensions.

Data availability

Data supporting this article have been included as part of the ESI.†

Conflicts of interest

There are no conflicts to declare.

Acknowledgements

C. D. C. acknowledges this material is based upon work supported by the National Science Foundation Graduate Research Fellowship Program under Grant No. DGE-1842165. N. E. W. and R. D. S. acknowledge support from the National Science Foundation under Grant No. MSN-1808590. R. D. S. acknowledges support from the U.S. Department of Energy, Office of Science, Office of Basic Energy Sciences, through Argonne National Laboratory under contract No. DE-AC02-06CH11357.

Work performed at the Center for Nanoscale Materials, a U.S. Department of Energy Office of Science User Facility, was supported by the U.S. DOE, Office of Basic Energy Sciences, under Contract No. DE-AC02-06CH11357. This work made use of the EPIC facility of Northwestern University's NUANCE Center, which has received support from the SHyNE Resource (NSF ECCS-2025633), the IIN, and Northwestern's MRSEC program (NSF DMR-1720139). This work made use of the EPIC facility of Northwestern University's NUANCE Center, which has received support from the SHyNE Resource (NSF ECCS-2025633), the IIN, and Northwestern's MRSEC program (NSF DMR-1720139). The submitted manuscript has been created by UChicago Argonne, LLC, Operator of Argonne National Laboratory ("Argonne"). Argonne, a U.S. Department of Energy Office of Science laboratory, is operated under Contract No. DE-ACO2-06CH11357. The U.S. Government retains for itself, and others acting on its behalf a paid-up nonexclusive, irrevocable worldwide license in said article to reproduce, prepare derivative works, distribute copies to the public, and perform publicly and display publicly, by or on behalf of the Government. The Department of Energy will provide public access to these results of federally sponsored research in accordance with the DOE Public Access Plan. https://awrgy.govidownloads/doe-public-access-plan.

References

1 K. A. Willets and R. P. Van Duyne, Localized Surface Plason Resonance Spectroscopy and Sensing, *Annu. Rev. Phys. Chem.*, 2007, **58**, 267–297.
2 E. S. Arinze, B. Qiu, G. Nyirjesy and S. M. Thon, Plasmonic Nanoparticle Enhancement of Solution Processed Solar Cells: Practical Limits and Opportunities, *ACS Photonics*, 2015, **3**, 158–173.
3 H. A. Atwater and A. Polman, Plasmonics for Improved Photovoltaic Devices, *Nat. Mater.*, 2010, 205–213.
4 F. Nan, S. J. Ding, L. Ma, Z. Q. Cheng, Y. T. Zhong, Y. F. Zhang, Y. H. Qiu, X. Li, L. Zhou and Q. Q. Wang, Plasmon Resonance Energy Transfer and Plexcitonic Solar Cell, *Nanoscale*, 2016, **8**(32), 15071–15078.
5 E. Cao, W. Lin, M. Sun, W. Liang and Y. Song, Exciton-Plasmon Coupling Interactions: From Principle to Applications, *Nanophotonics*, 2018, 145–167.
6 B. Luk'Yanchuk, N. I. Zheludev, S. A. Maier, N. J. Halas, P. Nordlander, H. Giessen and C. T. Chong, The Fano Resonance in Plasmonic Nanostructures and Metamaterials, *Nat. Mater.*, 2010, **9**(9), 707–715.
7 A. E. Schlather, N. Large, A. S. Urban, P. Nordlander and N. J. Halas, Near-Field Mediated Plexcitonic Coupling and Giant Rabi Splitting in Individual Metallic Dimers, *Nano Lett.*, 2013, **13**(7), 3281–3286.
8 R. Adato, A. Artar, S. Erramilli and H. Altug, Engineered Absorption Enhancement and Induced Transparency in Coupled Molecular and Plasmonic Resonator Systems, *Nano Lett.*, 2013, **13**(6), 2584–2591.
9 M. Moskovits, Surface-Enhanced Spectroscopy, *Rev. Mod. Phys.*, 1985, **57**(3), 783–826.
10 M. Osawa, Surface-enhanced infrared absorption, in *Near-Field Optics and Surface Plasmon Polaritons*, Springer, Berlin, 2001, pp. 163–187.
11 G. C. Schatz and R. P. V. D. Duyne, Electromagnetic mechanism of surface-enhanced spectroscopy, *Surface-Enhanced Vibrational Spectroscopy*, 2002, pp. 1–16.
12 S. Schlücker, Surface-Enhanced Raman Spectroscopy: Concepts and Chemical Applications, *Angew. Chem., Int. Ed.*, 2014, **53**(19), 4756–4795.
13 B. Sepúlveda, P. C. Angelomé, L. M. Lechuga and L. M. Liz-Marzán, LSPR-Based Nanobiosensors, *Nano Today*, 2009, 244–251.
14 S. K. Vashist, Point-of-Care Diagnostics: Recent Advances and Trends, *Biosensors*, 2017, **7**(62), 1–4.
15 K. L. Kelly, E. Coronado, L. L. Zhao and G. C. Schatz, The Optical Properties of Metal Nanoparticles: The Influence of Size, Shape, and Dielectric Environment, *J. Phys. Chem. B*, 2003, **107**(3), 668–677.
16 M. Brust, M. Walker, D. Bethell, D. J. Schiffrin and R. Whyman, Synthesis of Thiol-Derivatised Gold Nanoparticles in a Two-Phase Liquid-Liquid System, *J. Chem. Soc., Chem. Commun.*, 1994, 801–802.
17 P. Ghosh, G. Han, M. De, C. K. Kim and V. M. Rotello, Gold Nanoparticles in Delivery Applications, *Adv. Drug Delivery Rev.*, 2008, **60**(11), 1307–1315.
18 S. Rana, A. Bajaj, R. Mout and V. M. Rotello, Monolayer Coated Gold Nanoparticles for Delivery Applications, *Adv. Drug Delivery Rev.*, 2012, **64**(2), 200–216.
19 L. Vigderman, B. P. Khanal, E. R. Zubarev, L. Vigderman, B. P. Khanal and E. R. Zubarev, Functional gold nanorods: synthesis, self-assembly, and sensing applications, *Adv. Mater.*, 2012, **4**(36), 4811–4841.
20 A. M. Alkilany, A. I. B. Yaseen, J. Park, J. R. Eller and C. J. Murphy, Facile Phase Transfer of Gold Nanoparticles from Aqueous Solution to Organic Solvents with Thiolated Poly(Ethylene Glycol), *RSC Adv.*, 2014, **4**(95), 52676–52679.
21 A. B. Serrano-Montes, D. Jimenez de Aberasturi, J. Langer, J. J. Giner-Casares, L. Scarabelli, A. Herrero and L. M. Liz-Marza, A general method for solvent exchange of plasmonic nanoparticles and self-assembly into SERS-active monolayers, *Langmuir*, 2015, **31**(33), 9205–9213.
22 J. O. Park, S. H. Cho, J. S. Lee, W. Lee and S. Y. Lee, A Foolproof Method for Phase Transfer of Metal Nanoparticles via Centrifugation, *Chem. Commun.*, 2016, **52**(8), 1625–1628.
23 M. Liu and P. Guyot-Sionnest, Mechanism of Silver(I)-Assisted Growth of Gold Nanorods and Bipyramids, *J. Phys. Chem. B*, 2005, **109**(47), 22192–22200.
24 A. Gole and C. J. Murphy, Seed-Mediated Synthesis of Gold Nanorods: Role of the Size and Nature of the Seed, *Chem. Mater.*, 2004, **16**(19), 3633–3640.
25 C. J. Murphy, T. K. Sau, A. M. Gole, C. J. Orendorff, J. Gao, L. Gou, S. E. Hunyadi and T. Li, Anisotropic Metal Nanoparticles: Synthesis, Assembly, and Optical Applications, *J. Phys. Chem. B*, 2005, **109**(29), 13857–13870.

26 B. Nikoobakht and M. A. El-Sayed, Preparation and Growth Mechanism of Gold Nanorods (NRs) Using Seed-Mediated Growth Method, *Chem. Mater.*, 2003, **15**(10), 1957–1962.
27 G. Grochola, I. K. Snook and S. P. Russo, Computational Modeling of Nanorod Growth, *J. Chem. Phys.*, 2007, **127**(19), 194707.
28 T. H. Chow, N. Li, X. Bai, X. Zhuo, L. Shao and J. Wang, Gold Nanobipyramids: An Emerging and Versatile Type of Plasmonic Nanoparticles, *Acc. Chem. Res.*, 2019, **52**, 2136–2146.
29 S. Link and M. A. El-Sayed, Size and Temperature Dependence of the Plasmon Absorption of Colloidal Gold Nanoparticles, *J. Phys. Chem. B*, 1999, **103**(21), 4212–4217.
30 V. Sebastián, S. K. Lee, C. Zhou, M. F. Kraus, J. G. Fujimoto and K. F. Jensen, One-Step Continuous Synthesis of Biocompatible Gold Nanorods for Optical Coherence Tomography, *Chem. Commun.*, 2012, **48**(53), 6654–6656.
31 L. Scarabelli, A. Sánchez-Iglesias, J. Pérez-Juste and L. M. Liz-Marzán, A "Tips and Tricks" Practical Guide to the Synthesis of Gold Nanorods, *J. Phys. Chem. Lett.*, 2015, **6**(21), 4270–4279.
32 D. K. Smith and B. A. Korgel, The Importance of the CTAB Surfactant on the Colloidal Seed-Mediated Synthesis of Gold Nanorods, *Langmuir*, 2008, **24**(3), 644–649.
33 D. K. Smith, N. R. Miller and B. A. Korgel, Iodide in CTAB Prevents Gold Nanorod Formation, *Langmuir*, 2009, **25**(16), 9518–9524.
34 A. S. D. S. Indrasekara, R. C. Wadams and L. Fabris, Ligand Exchange on Gold Nanorods: Going Back to the Future, *Part. Part. Syst. Charact.*, 2014, **31**(8), 819–838.
35 S. Kittler, S. G. Hickey, T. Wolff and A. Eychmüller, Easy and Fast Phase Transfer of CTAB Stabilised Gold Nanoparticles from Water to Organic Phase, *Z. Phys. Chem.*, 2015, **229**(1–2), 235–245.
36 M. Lista, D. Z. Liu and P. Mulvaney, Phase Transfer of Noble Metal Nanoparticles to Organic Solvents, *Langmuir*, 2014, **30**(8), 1932–1938.
37 D. Gentili, G. Ori and M. Comes Franchini, Double Phase Transfer of Gold Nanorods for Surface Functionalization and Entrapment into PEG-based Nanocarriersw, *Chem. Commun.*, 2009, **39**, 5874–5876.
38 A. S. D. S. Indrasekara, R. C. Wadams and L. Fabris, Ligand Exchange on Gold Nanorods: Going Back to the Future, *Part. Part. Syst. Charact.*, 2014, **31**(8), 819–838.
39 D. Chateau, A. Liotta, F. Vadcard, J. R. G. Navarro, F. Chaput, J. Lermé, F. Lerouge and S. Parola, From Gold Nanobipyramids to Nanojavelins for a Precise Tuning of the Plasmon Resonance to the Infrared Wavelengths: Experimental and Theoretical Aspects, *Nanoscale*, 2015, **7**(5), 1934–1943.
40 M. M. Abdul-Moqueet, L. Tovias, P. Lopez and K. M. Mayer, Synthesis and Bioconjugation of Alkanethiol-Stabilized Gold Bipyramid Nanoparticles, *Nanotechnology*, 2021, **32**(22), 225601.
41 D. Chateau, A. Liotta, F. Vadcard, J. R. G. Navarro, F. Chaput, J. Lermé, F. Lerouge and S. Parola, From Gold Nanobipyramids to Nanojavelins for a Precise Tuning of the Plasmon Resonance to the Infrared Wavelengths: Experimental and Theoretical Aspects, *Nanoscale*, 2015, **7**, 1934–1943.